Contribution from the Chemistry Division, Argonne National Laboratory, Argonne, Illinois 60439, and the Department of Chemistry, University of Missouri, Columbia, Missouri 65211

Infrared and Raman Spectra of the Fluoroxysulfate Ion, SO_4F^-, and of Fluorine Perchlorate, ClO_4F[1]

EVAN H. APPELMAN,*[2a] LOUIS J. BASILE,[2a] and HYUNYONG KIM[2b]

Received October 23, 1981

The infrared and Raman spectra of solid cesium and rubidium fluoroxysulfates, $CsSO_4F$ and $RbSO_4F$, have been measured, along with the gas-phase spectra of the isoelectronic molecule fluorine perchlorate, ClO_4F. The spectra are consistent with a perchloric acid type structure of C_s symmetry, and the vibrational bands have been assigned with reference to the analogous species of C_{3v} symmetry: the fluorosulfate ion, SO_3F^-, and perchloryl fluoride, ClO_3F. Normal-coordinate analyses have been carried out for both ClO_4F and SO_4F^-.

Introduction

Appelman et al. have recently reported the preparation of the rubidium and cesium salts of the fluoroxysulfate ion, SO_4F^-. These are the only known ionic hypofluorites.[3a] The infrared and Raman spectra of these salts were noted to be similar to those of the isoelectronic species ClO_4F, fluorine perchlorate,[3b,c] and its homologues ClO_4Cl and ClO_4Br.[4] A subsequent X-ray diffraction study of $RbSO_4F$ has shown the SO_4F^- anion to have highly distorted tetrahedral coordination, with each sulfur atom bound to four oxygens, one of which is also bound to a fluorine atom.[5] The average length of the S=O double bond was found to be 1.434 Å, while the length of the S—OF single bond was found to be 1.652 Å. The crystal and site symmetries are respectively C_1 and C_1, while the molecular point group is C_s. The structures of ClO_4F, ClO_4Cl, and ClO_4Br have not been determined, but their chemical properties support their formulation as hypohalites,[6-8] while their molecular spectra can only be explained in terms of covalent perchlorate-related structures of C_s symmetry.[3b,c,4]

In this paper we present and analyze the infrared and Raman spectra of solid $RbSO_4F$ and $CsSO_4F$. Since reliable band assignments for the fluoroxysulfate ion require comparison with the isoelectronic ClO_4F, whose complete molecular spectra have not been published,[9] we also present and analyze the infrared and Raman spectra of gaseous ClO_4F. We have assigned the fundamental vibrations of these compounds with reference to those of the related species of C_{3v} symmetry:[10,11] the fluorosulfate ion, SO_3F^-, and perchloryl fluoride, ClO_3F. Normal-coordinate analyses have been carried out to corroborate the spectral assignments.

Experimental Section

Cesium and rubidium fluoroxysulfates were prepared by passing fluorine (20% in nitrogen) through solutions of the corresponding sulfates at −5 °C, followed by filtering, washing the precipitates with ice water, and drying first in an inert-gas stream and then in vacuo.

Fluorine perchlorate was prepared by circulating fluorine gas at 300-torr pressure through 73% perchloric acid in a Kel-F U-tube at 55 °C. A diaphragm pump with Viton diaphragm and valves was used to maintain the circulation. The product was passed through a Kel-F U-tube cooled to −78 °C to remove water and was collected in another U-tube cooled to −183 °C. It was purified by fractional distillation, and its purity was verified by mass spectrometry.

Infrared spectra were measured with a Beckman IR 4260 spectrometer, except for the $CsSO_4F$ spectrum between 350 and 450 cm^{-1}, for which a Beckman IR-11 spectrophotometer was used. The fluoroxysulfate salts attacked most window materials, making it necessary to use an unconventional technique. A diamond anvil cell was used in conjunction with 4× beam condenser.[12] The spectra of gaseous ClO_4F were measured in a Monel gas cell that was fitted with AgCl or fluorine-treated polyethylene windows and had a light path of 10 cm. Fluorine perchlorate was condensed into a side arm attached to the cell, and the pressure in the cell was varied by changing the temperature of the side arm. The very highest ClO_4F pressures, however, were determined by the total quantity of sample introduced into the cell.

Raman spectra were measured with a Spex 1401 monochromator linear in wavenumber and an RCA C31034 photomultiplier tube. Excitation was with a Coherent Radiation Model 52 argon ion laser. Fluoroxysulfate samples were sealed in Pyrex capillaries that were rotated during the measurements. Fluorine perchlorate samples were sealed in Pyrex ampules. Polarization measurements were made by method no. IV of those described by Claassen, Selig, and Shamir.[13] Fluoroxysulfate decomposes rapidly in aqueous solution,[3a] and because of this no attempt was made to obtain polarization data for the SO_4F^- vibrations.

Results and Discussion

Figure 1 shows the Raman spectrum of gaseous ClO_4F. For a molecule with C_s symmetry, we expect a total of twelve fundamental vibrations, all of which should be active both in the infrared and in the Raman. Eight of these modes belong to species A′ and should be polarized in the Raman spectrum, while the remaining four belong to species A″ and should be depolarized. Some of the ClO_3 stretches and deformations can be readily identified in reference to the known ClO_3F assignments,[11] as is shown in Table I. The polarized A′ species of the asymmetric ClO_3 stretches and deformations are not observed in our Raman spectra. The in-plane and out-of-plane ClO_3 rocking fundamentals ν_{11} and ν_7 are found to be nearly degenerate. We assign the polarized 888- and 678-cm^{-1} bands to the O—F and O—Cl stretches, respectively. The polarized band at 240 cm^{-1} is assigned to the Cl—O—F bend, while the depolarized band at 100 cm^{-1} is assigned to the O=Cl—O—F torsion. The depolarized shoulder at 220 cm^{-1} is probably caused by an impurity.

Figure 2 shows the infrared spectrum of gaseous ClO_4F. All of the vibrations assigned in the Raman spectrum are also found in the infrared, with the exception of ν_{12}, which is too low in frequency to be observable on our instrument. An

(1) Work supported by the U.S. Department of Energy, Division of Chemical Sciences, under Contract W-31-109-Eng-38.
(2) (a) Argonne National Laboratory. (b) University of Missouri.
(3) (a) Appelman, E. H.; Basile, L. J.; Thompson, R. C. *J. Am. Chem. Soc.* **1979**, *101*, 3384. (b) Agahigian, H.; Gray, A. P.; Vickers, G. D. *Can. J. Chem.* **1962**, *40*, 157. (c) Macheteau, Y.; Gillardeau, J. *Bull. Soc. Chim. Fr.* **1969**, 1819.
(4) Christe, K. O.; Schack, C. J.; Curtis, E. C. *Inorg. Chem.* **1971**, *10*, 1589.
(5) Gebert, E.; Appelman, E. H.; Reis, A. H., Jr. *Inorg. Chem.* **1979**, *18*, 2465.
(6) Schack, C. J.; Christe, K. O. *Inorg. Chem.* **1979**, *18*, 2619.
(7) Schack, C. J.; Pilipovich, D. *Inorg. Chem.* **1970**, *9*, 1387.
(8) Schack, C. J.; Christe, K. O.; Pilipovich, D.; Wilson, R. D. *Inorg. Chem.* **1971**, *10*, 1078.
(9) However, a thorough study of the molecular spectra of ClO_4F is currently in preparation: Christe, K. O.; Curtis, E. C. *Inorg. Chem.*, in press.
(10) Gillespie, R. J.; Robinson, E. A. *Can. J. Chem.* **1962**, *40*, 644.
(11) (a) Claassen, H. H.; Appelman, E. H. *Inorg. Chem.* **1970**, *9*, 622. (b) Clark, R. J. H.; Rippon, D. M. *Mol. Phys.* **1974**, *28*, 305. (c) Murphy, W. F.; Sunder, S.; Katz, H. *J. Raman Spectrosc.* **1978**, *7*, 76.
(12) Ferraro, J. R.; Basile, L. J. *Am. Lab. (Fairfield, Conn.)* **1979**, *11* (3), 31.
(13) Claassen, H. H.; Selig, H.; Shamir, J. *Appl. Spectrosc.* **1969**, *23*, 8.

0020-1669/82/1321-2801$01.25/0

Table I. Observed and Calculated Fundamentals (cm^{-1}) of Gaseous ClO_4F

ClO_3F[a]		ClO_4F				
species (C_{3v})	Raman	species (C_s)	Raman	IR	calcd	mode descriptions
E	1318	A″ ν_9	1300 dp	1300	1306	} asym ClO_3 str
		A′ ν_1	...	1300	1291	
A_1	1060	A′ ν_2	1050 p	1048	1053	sym ClO_3 str
		A′ ν_3	888 p	883	885	O–F str
A_1	716	A′ ν_4	678 p	674	672	Cl–O str
A_1	549	A′ ν_5	...	601	598	sym ClO_3 def
E	590	A″ ν_{10}	550 dp	565	565	} asym ClO_3 def
		A′ ν_6	532 p	530	530	
E	404	A″ ν_{11}	382 dp (?)	375	389	out-of-plane FO–ClO_3 rock
		A′ ν_7	378 p	375	382	in-plane FO–ClO_3 rock
		A′ ν_8	240 p	242	242	in-plane Cl–O–F bend
		A″ ν_{12}	100 dp	...	100	out-of-plane FO–ClO_3 torsion

[a] Reference 11c.

Table II. Infrared Overtone and Combination Bands of ClO_4F

freq, cm^{-1}	rel intens	assignt	freq, cm^{-1}	rel intens	assignt
201	m	$2\nu_{12}$	1610	w	$\nu_2 + \nu_{10}$
284	m	$3\nu_{12}$	1650	w	$\nu_2 + \nu_5$
750	m	$2\nu_{11}, 2\nu_7, \nu_6 + \nu_8$	1754	m	$2\nu_3$
945	w	$\nu_{10} + \nu_{11}, \nu_{10} + \nu_7$	1900	w	$\nu_1 + \nu_5, \nu_9 + \nu_5$
980	vw	$\nu_5 + \nu_{11}, \nu_5 + \nu_7$	1976	m	$\nu_9 + \nu_4$
1130	w	$2\nu_{10}$	2089	m	$2\nu_2$
1200	m	$2\nu_5$	2180	w	$\nu_1 + \nu_3, \nu_9 + \nu_3$
1380	m	$2\nu_4$	2337	s	$\nu_1 + \nu_2, \nu_9 + \nu_2$
1485	w	$\nu_3 + \nu_5$	2593	m	$2\nu_1, 2\nu_9, \nu_1 + \nu_9$
1550	w	$\nu_3 + \nu_4$			

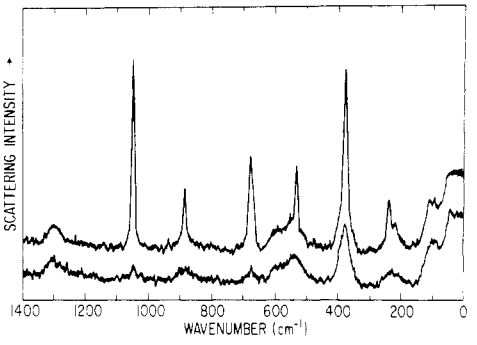

Figure 1. Raman spectrum of gaseous ClO_4F at ca. 2 atm and room temperature. The upper trace is with the electric vector perpendicular to the plane of the sample and slit length; the lower trace is with the electric vector parallel to this plane. Excitation is with the 4879-Å laser line, and the spectral band-pass is 10 cm^{-1}.

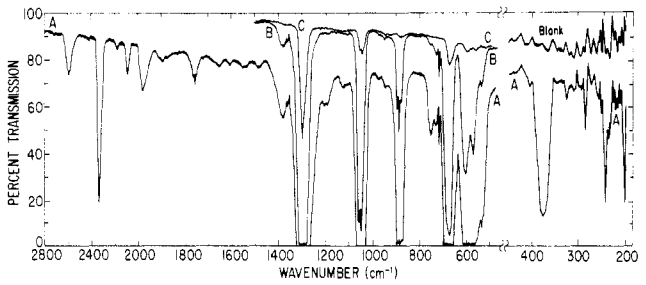

Figure 2. Infrared spectrum of gaseous ClO_4F at room tempeature: (A) 200 torr; (B) 15 torr; (C) 0.5 torr. The slit program is 2 times the standard. A blank spectrum at low wavenumber was run on the same cell after removal of the sample; the structure in it probably results from attack by the sample on the polyethylene windows.

additional infrared band is observed at 601 cm^{-1} and is assigned to ν_5. The band at 1300 cm^{-1} is very strong in the infrared, and we suspect that it contains both ν_1 and ν_9. A similar suggestion has been made in the interpretation of the infrared spectrum of ClO_4Cl.[4] The sharp feature at 715 cm^{-1} probably

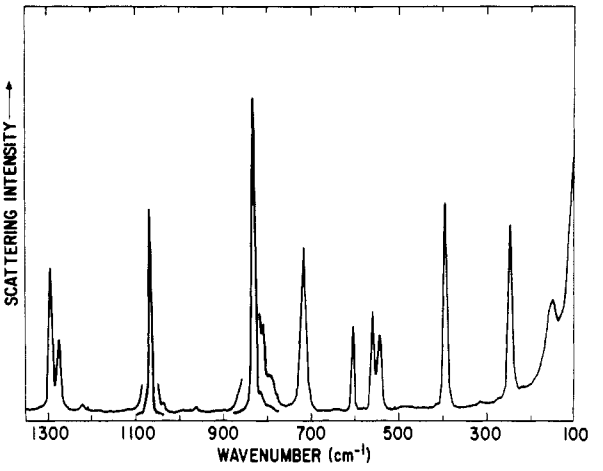

Figure 3. Raman spectrum of solid $RbSO_4F$. Peaks at 830 and 1067 cm^{-1} have been reduced by a factor of 5. Excitation is with the 5145-Å laser line, and the spectral band-pass is 5 cm^{-1}.

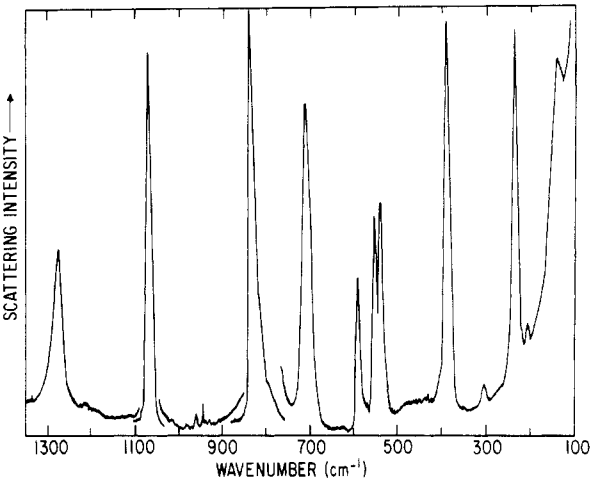

Figure 4. Raman spectrum of solid $CsSO_4F$. Peaks at 827 and 1061 cm^{-1} have been reduced by a factor of 4.5. Excitation is with the 5145-Å laser line, and the spectral band-pass is 5 cm^{-1}.

belongs to an impurity. The combination and overtone bands observed in the infrared spectrum are listed in Table II, along with suggested assignments. Expecially notable are the sharp bands at 201 and 284 cm^{-1}, which we assign to overtone bands of ν_{12}.

Figures 3 and 4 show the Raman spectra of $RbSO_4F$ and $CsSO_4F$, respectively. They are almost identical. The $RbSO_4F$ spectrum is used in the following discussion. As in the case of ClO_4F, we have assigned the SO_3 stretches and deformations in reference to the corresponding species of C_{3v} symmetry, in

Table III. Observed and Calculated Fundamentals (cm^{-1}) of Solid $RbSO_4F$ and $CsSO_4F$

SO_3F^- [a]		SO_4F^- compds						
species (C_{3v})	IR	species (C_s) [b]	$RbSO_4F$ Raman	$RbSO_4F$ IR	$CsSO_4F$ Raman	$CsSO_4F$ IR	calcd	ped [c]
E	1230	A'' ν_9	1294	1290	1278	1285	1294	$0.88K_1 + 0.04H_1 + 0.03H_2$
		A' ν_1	1273	1290	1278	1285	1273	$0.93K_1 + 0.05H_1$
A_1	1082	A' ν_2	1067	1065	1061	1063	1067	$0.88K_1 + 0.05K_2$
		A' ν_3	830	828	827	824	829	$0.71K_3 + 0.12H_4 + 0.10H_2$
A_1	786	A' ν_4	718	715	714	710	709	$0.53K_2 + 0.14H_4 + 0.10K_1 + 0.07H_1$
A_1	566	A' ν_5	605	598	597	589	608	$0.51H_1 + 0.009H_4 + 0.08H_3 + 0.08f_1$
E	592	A'' ν_{10}	560	560	558	555	560	$0.92H_1 + 0.06K_1$
		A' ν_6	545		545		540	$0.65H_1 + 0.13H_4 + 0.08K_2 + 0.08H_3$
E	405	A'' ν_{11}	396	397	393	394	396	$0.89H_3 + 0.08T$
		A' ν_7					388	$0.50H_2 + 0.19K_3 + 0.14K_2 + 0.11H_3$
		A' ν_8	246		239		243	$0.52H_4 + 0.19H_3 + 0.19K_2 + 0.13H_1$
		A'' ν_{12}	150		143		150	$0.92T + 0.08H_3$

[a] Reference 7. [b] Descriptions of vibrations are the same as for ClO_4F (Table I). [c] Potential energy distribution: relative contributions of valence force constants to the potential energy of the vibrational mode.

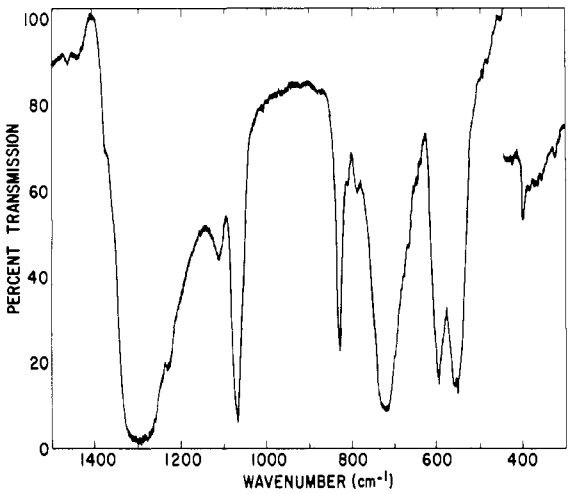

Figure 5. Infrared spectrum of solid $RbSO_4F$.

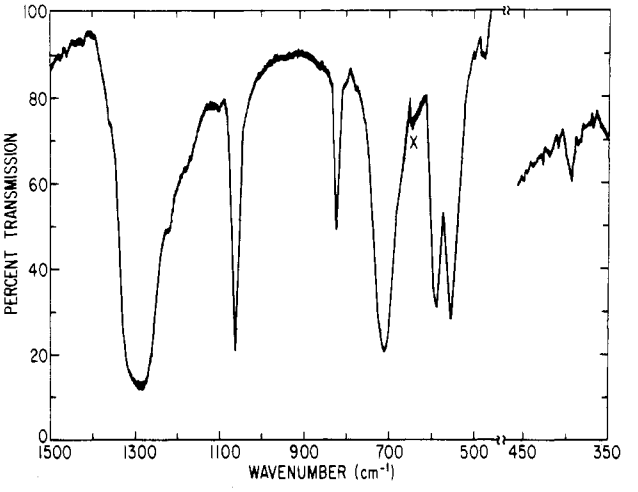

Figure 6. Infrared spectrum of solid $CsSO_4F$. X indicates an instrumental artifact.

this case the fluorosulfate anion, SO_3F^-.[10] The resulting assignments are given in Table III. The frequencies are comparable to those of the corresponding vibrations of ClO_4F. The polarized bands at 830 and 710 cm^{-1} are assigned respectively to the O–F stretch, ν_3, and the S–O stretch, ν_4. Only one SO_3 rocking band is observed: at 396 cm^{-1}. The rocking modes in ClO_4F are nearly degenerate, and we have assumed that they are unresolved in the case of SO_4F^-. We have assigned the 246- and 150-cm^{-1} bands to the ν_8 and ν_{12} modes by analogy with the ClO_4F assignments. Small unassigned bands at 210 and 310 cm^{-1}, which are most apparent in the Raman spectrum of $CsSO_4F$, persist after thermal decomposition of the sample and are probably caused by impurities. The satellite bands observable on the low-frequency side of ν_3 may also be due to impurities, or they may result from combinations with lattice modes.

Figures 5 and 6 show the infrared spectra of $RbSO_4F$ and $CsSO_4F$. The quality is not as good as in the Raman spectra, because of the energy loss that results from use of the diamond cell. However, most of the fundamental vibrations that were assigned in the Raman spectra are also found in the infrared. Notably, the band at 1290 cm^{-1} is unresolved, and the ν_6 band at 545 cm^{-1} is not resolved from the ν_{10} band at 560 cm^{-1}. The weak band at 1105 cm^{-1} probably comes from an impurity.

In our normal-coordinate analysis[14] we have made use of the crystallographic bond distances and angles in fluoroxysulfate. Average values were used for the S=O distance and the O=S=O angle. In the case of ClO_4F we have assumed that its distorted-tetrahedral perchlorate structure is the same as that of $HClO_4$[15] and that the O–F bond distance and Cl–O–F bond angle are the same as the O–F bond distance and S–O–F bond angle in fluoroxysulfate, namely, 1.41 Å and 108°. After a few trial and error adjustments of valence force constants, it became apparent that a single O=Cl—O bending constant could not predict the nearly degenerate ClO_3 rocking fundamentals ν_{11} and ν_7. We have therefore used two different

Table IV. Valence Force Constants Used To Calculate the Fundamental Frequencies Given in Tables I and III[a]

	ClO_4F	SO_4F^-
K_1(X=O)	9.30	8.56
K_2(X–O)	1.80	2.40
K_3(O–F)	3.40	2.85
H_1(O=X=O)	1.92	1.85
H_2(O=X–O in plane)	1.90	1.90
H_3(O=X–O out of plane)	1.00	1.00
H_4(X–O–F)	1.70	1.55
T(O=X–O–F)	0.03	0.067
$f_1(H_1,H_4)$	0.50	0.50
$f_2(K_1,K_2)$	1.50	0.0
$f_3(K_3,H_4)$	0.0	−0.30

[a] Force constant units: bond stretch K and interaction f_2 in mdyn/Å; bend H, torsion T and interaction f_1 in mdyn Å/rad²; interaction f_3 in mdyn/rad. X stands for Cl or S atoms.

(14) For a description of the computer program used, see: Kim, H. *Biopolymers*, in press.

(15) Clark, A. H.; Beagley, B.; Cruickshank, D. W. J.; Hewitt, T. G. *J. Chem. Soc. A* **1970**, 1613.

bending constants: the in-plane constant H_2 and the out-of-plane constant H_3. We have proceeded in a similar fashion with SO_4F^-. In addition, we have introduced three interaction constants to improve the agreement between the calculated and observed frequencies. The calculated frequencies are included in Tables I and III, and the corresponding valence force constants are listed in Table IV. Also included in Table III are the computed potential energy distributions for SO_4F^-. These indicate the relative contributions of the various force constants to the potential energy of each of the fundamental vibrations. (Separate potential energy distributions for ClO_4F are not given in Table I, since the dynamics of the two isoelectronic molecules are essentially the same.)

Normal-mode descriptions given in Table I for ClO_4F are equally applicable to SO_4F^-. The descriptions of the deformation modes are given in reference to ClO_3F and SO_3F^-. These descriptions are only approximate for the less symmetrical species ClO_4F and SO_4F^-. Thus the ν_5, ν_6, and ν_{10} modes of ClO_4F bear some resemblance to both the symmetrical (A_1) and the asymmetrical (E) deformation modes of ClO_3F. We have assigned ν_5 to the symmetrical deformation, because its normal motions appear to be more symmetrical than those of ν_6.

From the X-ray data we know that the SO_4F^- ion has a perchloric acid like structure, while the 1:1 correspondence that we find in the vibrational assignments of ClO_4F and SO_4F^- is consistent with a close structural resemblance between these two isoelectronic species. The valence force constants governing the motions of the ClO_3 and SO_3 moieties are essentially the same, as can be seen from Table IV, but notable differences are evident between the force constants for the O—F stretch and the O=X—O—F torsion in the two molecules. The observed frequencies are 888 and 100 cm^{-1} for ClO_4F and 830 and 150 cm^{-1} for SO_4F^-, and the two vibrations are fairly pure valence modes. We may attribute the differences to the negative charge on the fluoroxysulfate ion, which will tend to increase the electron densities on the ligand atoms. Such increased electron density in the O—F bond would be expected to lower the O—F force constant and increase the repulsion between the O—F and S=O bonds. The latter would be reflected in a stronger O=S—O—F torsion constant. Fluorine NMR data do, in fact, indicate an electron density around the fluorine in SO_4F^- greater than around that in ClO_4F.[3a,b]

It is very interesting to observe that in both SO_4F^- and ClO_4F the XO_3 rocking modes ν_{11} and ν_7 are nearly degenerate. In a pure valence force field model, we would expect the asymmetry introduced by the O—F group to split the ν_{11} and ν_7 bands by 50–100 cm^{-1}. To account for the near degeneracy in our normal-mode calculations, which assume harmonic force fields, we were forced to introduce two different O=X—O bending constants, H_2 and H_3 (see Table IV). A truer picture is probably that the low-frequency modes of X—O—F bending, ν_8, and O=X—O—F torsion, ν_{12}, are strongly coupled to the XO_3 rocking modes.

Acknowledgment. We wish to thank Dr. Karl Christe for helpful discussions of the spectral assignments and for making available to us his spectroscopic data on ClO_4F prior to publication.

Registry No. $CsSO_4F$, 70806-67-6; $RbSO_4F$, 70631-32-2; ClO_4F, 10049-03-3.

Contribution from the Chemical Crystallography Laboratory, Oxford University, Oxford, OX1 3PD, England, the Department of Chemistry, University of Missouri—Rolla, Rolla, Missouri 65401, and the Nuclear Physics Division, Atomic Energy Research Establishment, Harwell, Didcot OX11 ORA, England

A Neutron Diffraction, Magnetic Susceptibility, and Mössbauer-Effect Study of the $(Mn_xFe_{1-x})_yO$ Solid Solutions

DAVID A. O. HOPE, ANTHONY K. CHEETHAM,* and GARY J. LONG*

Received August 24, 1981

A total of 14 mixed-metal oxides, $(Mn_xFe_{1-x})_yO$, with x ranging from zero to 0.975 and y ranging from 0.910 to 0.998, have been prepared. Chemical analysis and powder neutron diffraction studies confirm that nonstoichiometry in these oxides is accommodated by the formation of defect clusters similar to those observed in Fe_yO. Magnetic susceptibility measurements from 50 to 300 K indicate that the Néel temperature decreases approximately linearly from ca. 200 K for Fe_yO to 142 K for $(Mn_{0.66}Fe_{0.34})_{0.954}O$. The room-temperature Mössbauer-effect spectra show the expected amount of high-spin iron(III) with isomer shifts in the range of 0.45 to 0.24 mm/s, decreasing with increasing manganese content. The high-spin iron(II) absorption in Fe_yO may be fitted with two quadrupole doublets with isomer shifts of ca. 1.00 and 0.95 mm/s and quadrupole interactions of ca. 0.42 and 0.80 mm/s respectively. The major new feature apparent upon the addition of manganese is a third quadrupole doublet with an isomer shift of ca. 1.05 mm/s and splittings in the range of 0.96 to 1.38 mm/s. The area-weighted average quadrupole interaction, which is ca. 0.6 mm/s for Fe_yO, increases slowly with increasing manganese content to a maximum of ca. 0.7 mm/s at 50% manganese. At higher levels of manganese, the area-weighted average quadrupole interaction drops sharply to a value of ca. 0.1 mm/s at 97.5% manganese. This behavior may be understood in terms of the number of defects present and the nature and distribution of the iron/manganese near-neighbor ions. The iron(II) isomer shift increases slightly from 0.95 to 1.10 mm/s with increasing manganese content.

Introduction

The monoxides of manganese and iron crystallize in the NaCl structure and accommodate nonstoichiometry by the oxidation of metal ions and the creation of cation vacancies. This is particularly marked in iron(II) oxide, which exists between the compositions $Fe_{0.95}O$ and $Fe_{0.88}O$ at 1000 °C and disproportionates below 570 °C.[1] The problem of the arrangement of defects in the equilibrium and quenched phases of this oxide has received a great deal of attention, and recent experimental[2-5] and theoretical[6] work suggests that the pre-

* To whom correspondence should be addressed: A.K.C., Oxford University; G.J.L., University of Missouri—Rolla.

(1) Fender, B. E. F.; Riley, F. D. *J. Phys. Chem. Solids* **1969**, *30*, 793.
(2) Andersson, B.; Sletnes, J. O. *Acta Crystallogr., Sect. A* **1977**, *A33*, 268.
(3) Greenwood, N. N.; Howe, A. T. *J. Chem. Soc., Dalton Trans.* **1972**, 110.
(4) Battle, P. D.; Cheetham, A. K. *J. Phys. C* **1979**, *12*, 337.

0020-1669/82/1321-2804$01.25/0